Investigation of the Heat Transfer Intensification Mechanism for a New Fluidized Catalyst Cooler

Xiuying Yao, Yongmin Zhang, and Chunxi Lu
State Key Laboratory of Heavy Oil Processing, China University of Petroleum, Beijing 102249, P.R. China

Xiao Han
Pressure Pipeline Division, China Special Equipment Inspection and Research Institute, Beijing 100029, P.R. China

DOI 10.1002/aic.14841
Published online April 28, 2015 in Wiley Online Library (wileyonlinelibrary.com)

A small cold model was employed to investigate the heat-transfer mechanism for a new fluidized catalyst cooler. Local heat-transfer coefficients (h) and tube surface hydrodynamics were systematically measured by a specially designed heat tube and an optical fiber probe. The higher total h further validated the feasibility of the heat transfer intensification method used in the new catalyst cooler, which indicated that the induced higher packet renewal frequency due to the nonuniform gas distribution played a dominant role in its increased hs. Strongest heat transfer intensification effect was located at $r/R_w>0.8$ below the heat transfer intensification height. The changes of the mean packet residence time in the radial and axial directions and with superficial gas velocity were all agreeable with the measured hs according to the packet renewal theory. This further demonstrated the feasibility of the experimental method for tube surface hydrodynamics. © 2015 American Institute of Chemical Engineers *AIChE J*, 61: 2415–2427, 2015
Keywords: intensification, heat transfer, bed-to-wall, fluidized bed, surface hydrodynamics, fluid catalytic cracking

Introduction

In petroleum refineries, fluid catalytic cracking (FCC) process is widely used for converting vacuum gas oil or heavier residue into lighter and more valuable hydrocarbon products.[1] It is one of the most important secondary oil conversion processes and usually the chief profit source of most refineries.[2,3] Heat balance is a key issue for FCC process in which the heat generated from coke-burning regeneration must balance the heat requirement by the reactor system where isothermal cracking reactions occur. When processing heavier carbon-containing residue feedstock, superfluous heat releases as a result of higher coke yield, which exceeds the requirement for heat balance. Therefore, it is necessary to add catalyst coolers to remove the superfluous heat. Otherwise, regenerator temperature will increase substantially, leading to a reduction in catalyst circulation rate (i.e., catalyst to oil ratio) and worsened product yields or even serious accidents.[4,5]

There are various types of catalyst coolers for FCC units.[6–14] Due to its higher heat-transfer efficiency, operating flexibility, and reliability, countercurrent dense-phase catalyst coolers is more widely found in petroleum refineries, where catalysts from one upper inlet flow downward and exit from a bottom outlet.[5] The macro solids flow direction is opposite to the fluidizing gas. There is usually a bubbling or turbulent flow regime in this type of catalyst cooler, so a high bed density can be maintained.

Correspondence concerning this article should be addressed to Y. Zhang at zym0876@gmail.com.

Although external catalyst coolers have been used in refineries for decades, many problems, such as lower cooling capacity than the designed value and heat tube leakage, are still frequently encountered.[15–19] Lower cooling capacity is usually related to bad fluidization quality inside an external catalyst cooler. Improper designs of gas distributor, heat tube configuration, and tube fins can all lead to possible bad fluidization quality, resulting gas-bypassing, local defluidization, gas streaming, and so forth.[20–23] Heat tube leakage may result from solids erosion, overheated tube, or thermal stress. Solids erosion usually happens near the upper solids inlet or results from improper gas distributor design. Due to different localized fluidization qualities, heat capacities of different tubes may differ considerably if their water circulation rates or heat-transfer coefficients or temperature differences are nonuniform. Most seriously, all the liquid water may be vaporized into over-heated steam if the high cooling capacity is very high, resulting in increased tube wall temperature. The resulted thermal stress may crack some tubes. If tube leakage happens, the damaged tubes have to be shut down, but the unit throughput usually has to decrease to maintain unit heat balance. Sometimes, the entire unit had to be shut down, resulting in serious economic loss. Therefore, heat transfer intensification technologies are very necessary and important. Herein, heat transfer intensification is not only related to increasing the heat-transfer capacity but also improving the equipment reliability.

In a countercurrent dense-phase external catalyst cooler, particle convection plays a dominant role than gas convection and radiation in bed-to-wall heat transfer.[24–26] There have been a lot of efforts on improving the performance of

various external catalyst coolers. Except for improving equipment reliability,[18,27,28] there are also various studies on increasing the cooling capacity of an external catalyst cooler.[29–35] There are three categories of methods according to the universal expression of the cooling capacity

$$q = hA_w(T_b - T_w) \quad (1)$$

that is, increasing (a) heat-transfer coefficient h, (b) contacting area A_w, and (c) temperature difference between heat-transfer surface and a fluidized bed ($T_b - T_w$).

In an industrial FCC external catalyst cooler, the temperature difference of heat transfer is changed by adjusting the solids circulation rate.[29] Increasing solids circulation rate raises the effluent solids temperature and thus increase the average temperature difference.[30] The heat-transfer area is increased by welding the vertical fins[31,32] or the short nail-shaped steel bars[33] on the tube surface. However, improper design of fins and bars not only limits lateral solids mixing and creates nonuniform distribution of cooling capacity among heat tubes,[34,35] but also deteriorates solids-wall contact due to stronger wall effect. Heat-transfer coefficient can be increased by changing the bed hydrodynamics and solids mixing properties, which involves optimized selections of superficial gas velocity, structural design, and layout of the heat tubes, gas distributor design and so on.

Numerous investigations had been carried out to study the bed-to-wall heat transfer in dense-phase fluidized beds like in external catalyst coolers.[36–46] Among these studies, only Stefanova et al.,[36,37] Di Natale et al.[44] and two our previous publications,[39,46] are directly related to bed-to-wall heat transfer in fluidized beds of Geldart A particles with immersed vertical heat tubes.

This study was a continuous job based on our two previous studies.[39,46] In Yao et al.,[39] a special electrically heated tube was designed to measure both axial and radial profiles of heat-transfer coefficient. It is found that the heat-transfer coefficient was almost not influenced by the axial height. In the radial direction, the heat-transfer coefficient kept constant in the bed center and decreased sharply when approaching to the bed wall. Moreover, an optical fiber probe was used to measure the tube surface hydrodynamics. Two important parameters, that is, mean packet residence time and packet fraction according to the packet renewal model,[40] were obtained by analyzing the particle concentration signal on heat tube surface. They found that the profiles of mean packet residence time were mostly agreeable with those of heat-transfer coefficient based on the packet renewal mechanism,[40] demonstrating the dominant role of packet renewal on bed-to-wall heat transfer.

In another study,[46] we proposed a new heat transfer intensification method for FCC external catalyst coolers to debottleneck the low cooling capacity existed in many industrial Resid FCC units. This method uses the idea of a recirculating fluidized bed to promote internal solids circulation and increase bed-to-wall heat-transfer coefficient.[47,48] Figure 1 shows a schematic of this idea. Similar to a recirculating fluidized bed, a double-distributor design is used in the bed bottom. A central distributor (preferred as a perforated plate distributor) provides a majority of fluidizing gas and an annular ring pipe distributor installed near the wall, slightly above the central distributor, only provides a minority of fluidizing gas. This results in higher voidage in the center and lower voidage near the wall. A density difference between the bed

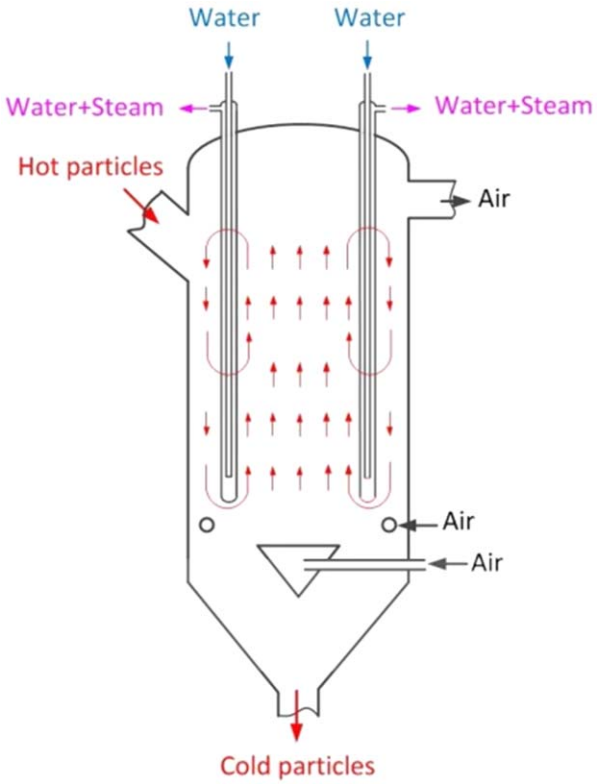

Figure 1. Schematic of the heat transfer intensification method.

[Color figure can be viewed in the online issue, which is available at wileyonlinelibrary.com.]

center and the near wall region creates a strong internal solids circulation pattern as shown in Figure 1, which is used to strength solids renewal on heat tube surfaces.

This method had been partially validated experimentally in a large cold model with finned vertical heat tubes similar to those in industrial FCC external catalyst coolers.[46] Figure 2 shows the schematics of the different gas distributor designs used by Yao et al.[46] for a traditional and a new annular external catalyst cooler using this heat transfer intensification method shown in Figure 1. The experimental results showed that the maximum heat-transfer coefficient of the new catalyst cooler was 9.5% higher than that of a traditional catalyst cooler. In other operating conditions, the increments on heat-transfer coefficient were more remarkable. Yao et al.[46] attributed the resultant heat transfer intensification to the design of the annular catalyst cooler. However, the double distributors in the annular catalyst cooler undoubtedly provided a more uniform gas distribution than the single ring pipe distributor in the base catalyst cooler, which was also helpful to fluidization quality and bed-to-wall heat transfer. Therefore, it remained doubtful whether the enhanced solids circulation or the improved initial gas distribution in the annular catalyst cooler played a more dominant role in the observed heat transfer intensification.

To clarify this doubt, a new fluidized cold model was built to study the heat transfer intensification mechanism in this study. A more uniform perforated plate distributor was used in the base catalyst cooler to exclude the influence of gas distribution. The effectiveness of this heat transfer intensification method can thus be verified more explicitly. The newly developed two methods for measuring local heat-transfer coefficient

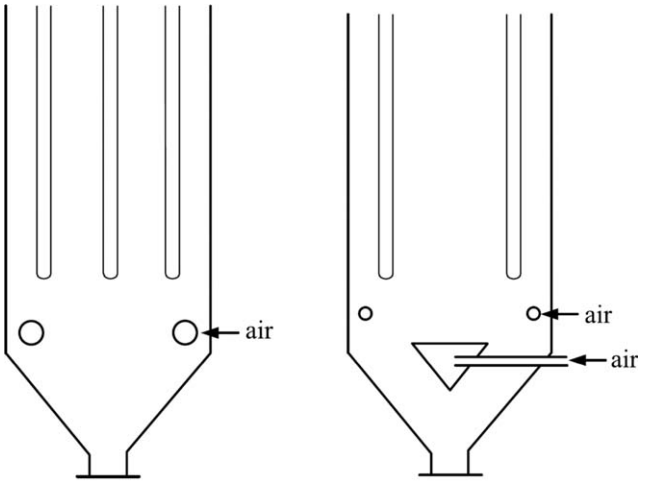

(a) Base catalyst cooler (b) Annular catalyst cooler

Figure 2. Schematic of the base (a) and new annular (b) catalyst coolers used in Yao et al.[46]

and tube surface hydrodynamics, which was described in more detail in our previous publication,[39] was reused to measure the axial and radial profiles of heat-transfer coefficient as well as the packet parameters on tube surfaces in the new annular catalyst cooler. By comparing these experimental results with those measured in the base catalyst cooler,[39] the heat transfer intensification regions can be more explicitly located. Moreover, the relationship between the changed heat-transfer coefficient and the hydrodynamics on heat tube surface can also be revealed more clearly. To facilitate readers' understanding, some contents in Yao et al.,[39] for example, some important data, equations, figures and descriptive texts were reused in the following content.

Experiment

Experimental setup

The experiment was implemented in a small-scale fluidized bed of ID 286 mm and height 6 m. FCC equilibrium catalysts (not fresh catalysts) of mean diameter 69.4 μm and particle density 1500 kg/m^3 were used as the fluidized particles, which had the same solids properties to those in industrial FCC catalyst coolers. During experiment, the static bed height was kept to be 1.1 m. Compressed air from a Roots blower was used as the fluidizing gas. The entrained particles were collected by two cyclone separators in series and then returned to the bed via their diplegs to maintain a constant particle inventory. A multisectional copper tube heated electrically was used to simulate a vertical heat tube in a FCC external catalyst cooler and measure the axial and radial profiles of heat-transfer coefficients. More details about the experiment unit were provided in Yao et al.[39]

Figure 3 shows the two external catalyst coolers used in this study, that is, a base catalyst cooler and a new annular catalyst cooler. It should be noted that the base catalyst cooler shown in Figure 3a is in fact a redrawn three-dimensional picture of the catalyst cooler studied in Yao et al.[39] It is the structure of the gas distributors that distinguishes the two catalyst coolers. The base catalyst cooler was used as a comparison reference. In the base catalyst cooler, a single perforated plate, which had an equal area to the bed cross section and an open area ratio of 0.9%, was used to distribute the fluidizing gas. Herein, the open area ratio is a parameter used to characterize a perforated plate distributor, which is defined as the total aperture area divided by the area of the plate distributor.

According to the idea of the new heat transfer intensification method, a double-distributor design, including a perforated plate distributor in the bed center and a ring pipe distributor near the wall, was used for gas distribution in the annular catalyst cooler. This perforated plate distributor had a smaller area, proximately half of the cross-sectional area of the bed. Its open area ratio was also 0.9%. The ring pipe distributor had a ring diameter of 256 mm and the ID of the pipe was 18 mm. There were 9 apertures of diameter 3 mm drilled on the pipe. Detailed information about the three different gas distributors is listed in Table 1. In this study, the gas volume flow rates from the perforated plate and ring pipe distributors divided by the cross-sectional area of the bed were defined as two superficial gas velocities, u_1 and u_2. The relationship between them and the actual superficial gas velocity of the annular catalyst cooler u, u_1, and u_2 is

$$u = u_1 + u_2 \tag{2}$$

The superficial gas velocity range in the base catalyst cooler was 0.1–0.5 m/s. The ranges of u_1 and u_2 in the annular catalyst cooler were 0.055–0.485 m/s and 0.015–0.045 m/s, respectively. It can be seen that the flow rate of gas through the central perforated plate distributor is proximately an order higher than that through the ring pipe distributor.

Comparatively, the initial gas distribution in the base catalyst cooler was more uniform than in the annular catalyst cooler. Therefore, its bed fluidization quality is expected to be better than in the annular catalyst cooler. This was different from the distributor design in our previous study,[46] where the new annular catalyst cooler had a more uniform gas distribution.

Measurement

The heat-transfer coefficient was the most important parameter measured in this study. A specially designed multisectional copper tube with electrical heating wires and thermocouples was used to measure the axial and radial profiles of heat-transfer coefficient. As shown in Figure 4, the vertical heat tube was composed of five heated sections, six insulation sections and two supported tubes. The five heated sections, made of copper, were used to measure the heat-transfer coefficients at different axial heights. From bottom to top, the five heated sections were named as Heater #1–Heater #5. The heat-transfer coefficients at different radial positions were measured by radially moving the heat tube. During experiment, the heat-transfer coefficient was determined by the following equation

$$h = \frac{q_{\text{in}}}{A_{\text{w}}(T_w - T_b)} = \frac{U_{\text{h}}^2/R_{\text{h}}}{A_{\text{w}}(T_w - T_b)} \tag{3}$$

Here, q_{in} is the input heat flux of the heating wire, U_{h} and R_{h} are the input voltage and the resistance of the heating wire, respectively. The contacting area between the copper tube surface and the bed material A_{w} is the area of the cylindrical surface of the copper tube. T_{w} and T_{b} are the measured heat tube wall temperature and the bed temperature, respectively. During the determination of h by Eq. 3, the conductive heat transferred from the two end surfaces of a cylindrical copper heater was actually neglected, leading to

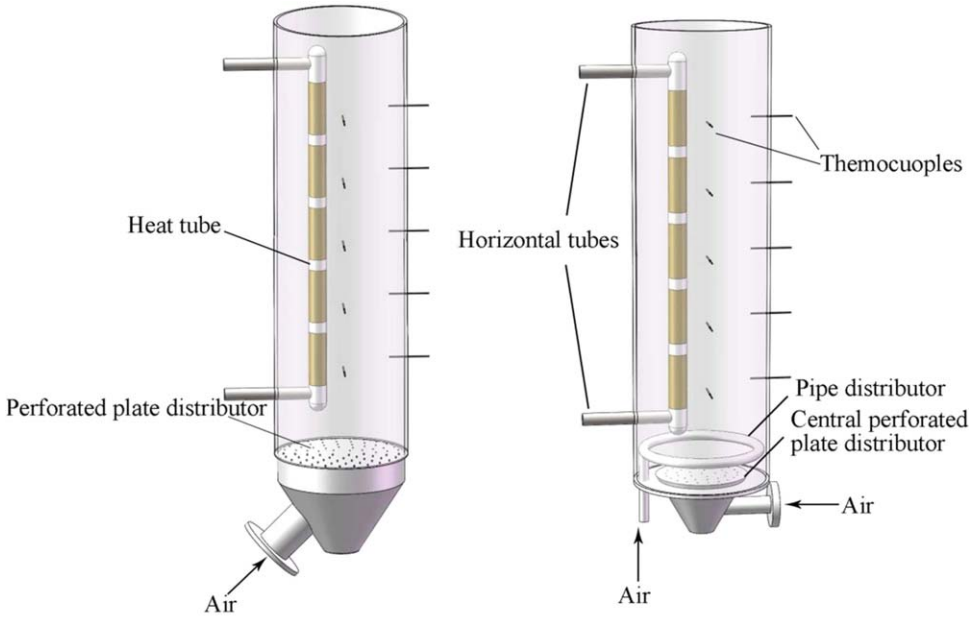

Figure 3. The two used catalyst coolers.

[Color figure can be viewed in the online issue, which is available at wileyonlinelibrary.com.]

an error in q_{in}. The error analysis of the measured heat-transfer coefficient had already been conducted and discussed in Yao et al.[39] Therein, a method was developed to estimate the error range of the measured heat-transfer coefficient. It was found that the relative errors were less than 3%, which demonstrated the actual heat loss from the two end surfaces was actually very small.

During experiment, q_{in} was kept equal under all tests. Therefore, higher measured heat-transfer coefficients were accompanied with lower temperature differences, and vice versa. The measurement positions for heat-transfer coefficient in this study are listed in Table 2. More details about the structural design of the heat tube, the calculation method of heat-transfer coefficient and the assessment of the measurement error can be found in Yao et al.[39]

Bed-to-wall heat transfer in fluidized beds is closely related to the gas-solids flow on the heat tube surface. To uncover the inner mechanisms corresponding to the different heat-transfer properties in the two catalyst coolers, tube surface hydrodynamics was also measured in this study by an optical fiber probe. During measurement, the optical fiber probe was inserted into a vertical stainless steel tube with same dimensions to the heat tube shown in Figure 4. In this study, its tip was aligned to the surface of the cylindrical surface of the tube. After determining a threshold voltage value of solids concentration, the transient particle concentration signals measured by the optical fiber probe was used to distinguish the two-phase flow structure on the heat tube surface, that is, the bubble and packet. Two important parameters based on the packet renewal model,[40] that is, the packet fraction and the mean packet residence time, were then determined by Eqs. 4 and 5

$$\delta_{pa} = \frac{\sum_{i=1}^{n} \tau_{pa,i}}{t} \tag{4}$$

and

$$\tau_{pa} = \left[\frac{\sum_{i=1}^{n} \tau_{pa,i}}{\sum_{i=1}^{n} \sqrt{\tau_{pa,i}}}\right]^2 \tag{5}$$

respectively. Here, $\tau_{pa,i}$ is the residence time of a packet passing through the probe tip and t is the total measurement period. According to the packet renewal model,[40] the mean packet residence time τ_{pa} in Eq. 5 is a root mean residence time. Its reciprocal is equivalent to packet renewal frequency, an indicator of the strength of solids renewal on heat tube surface.

Our previous study had shown that the predicted heat-transfer coefficients based on the determined packet parameters by this method could be qualitatively agreeable with the measurement results. More details about the optical fiber probe, its arrangement during measuring tube surface hydrodynamics, and the analyzing method to determine the two packet parameters can be found in Yao et al.[39]

In a bubbling fluidized heat exchanger, particle concentration increases as approaching to the heat tube due to the

Table 1. Geometry Parameters of the Three Gas Distributors

Type	Size	Plate Diameter (mm)	Ring Diameter (mm)	Pipe ID (mm)	Open Area Ratio	Aperture Number	Aperture ID (mm)
Base catalyst cooler	Plate distributor	286	–	–	0.9%	82	3
Annular catalyst cooler	Plate distributor	200	–	–	0.9%	40	3
	Ring pipe distributor	–	256	18	–	9	3

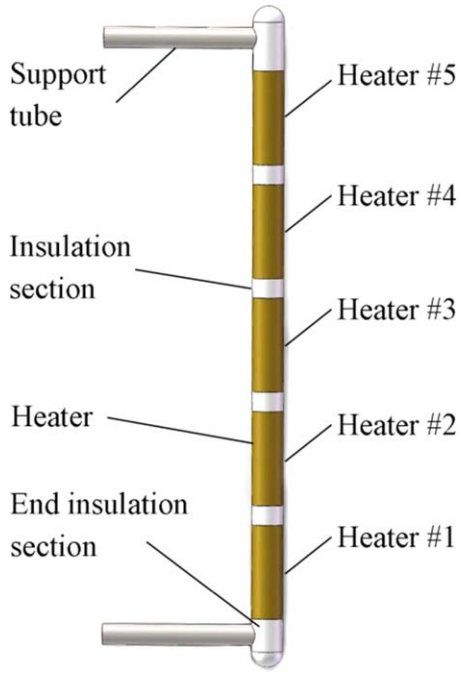

Figure 4. Schematic of the heat tube.

[Color figure can be viewed in the online issue, which is available at wileyonlinelibrary.com.]

wall effect. According to the measured particle concentration in Figure 5a, Yao et al.[39] found a solids static layer of thickness 3–8 mm on the tube surface of the base catalyst cooler. In this study, the thickness of the solids static layer on the tube surface of the new annular catalyst cooler was also determined in a same method. Figure 5b shows the measured particle concentrations. It is found that a very small protruding of the probe tip can make the measured particle concentration drop considerably. According to Figure 5b, the thickness of the solids static layer in the annular catalyst cooler should be 0–3 mm, which is smaller than in the base catalyst cooler. A smaller thickness of the solids static layer indicates weaker heat resistance and higher heat-transfer coefficient. In the annular catalyst cooler, the double-distributor design makes internal solids circulation more strongly and solids renewal on tube surface more frequently. This is believed to be the cause of the smaller thickness of solids static layer in the annular catalyst cooler. In the following content, this point can be further verified by the experimental results of heat-transfer coefficient and bed hydrodynamics.

Results and Discussion

Comparison of the average heat-transfer coefficient

Figure 6 compares the total heat-transfer coefficients of the two catalyst coolers averaged from different radial and axial positions by Eqs. 6 and 7

$$\overline{h_{\mathrm{ri}}} = \int_0^{R_i} 2h(r)rdr/{R_i}^2 \tag{6}$$

$$\overline{h_{\mathrm{m}}} = (\overline{h_{r1}}+\overline{h_{r2}}+\overline{h_{r3}}+\overline{h_{r4}}+\overline{h_{r5}})/5 \tag{7}$$

Here, $\overline{h_{\mathrm{ri}}}$ is the area-averaged heat-transfer coefficient at an axial height, $\overline{h_{\mathrm{m}}}$ is the total heat-transfer coefficient. It is found that, under most operating conditions, the heat-transfer coefficients in the annular catalyst cooler are higher than those

Table 2. Measurement Positions Along the Axial and Radial Directions

Measured positions	Value
Axial direction, z (m)	0.222, 0.367, 0.512, 0.657, 0.802
Radial direction, r/R_{w}	0.0, 0.3, 0.6, 0.8, 0.9, 0.95

in the base catalyst cooler. It is increment of heat-transfer coefficient than the base catalyst cooler increases with increasing superficial gas velocity. Moreover, the heat-transfer coefficients of the annular catalyst cooler can be further increased by increasing the ratio of the gas flow rate from the ring pipe distributor near the column wall, approximately 4% increment obtainable. This indicates that the ratio of the flow rates from the two gas distributors in the annular catalyst cooler adds a new means to adjust the cooling capacity of the annular catalyst cooler. In this study, the maximum increment of heat-transfer coefficient is obtained at u=0.5 m/s and u_2=0.045 m/s in the annular catalyst cooler, which is 15.5% higher than the corresponding heat-transfer coefficient in the base catalyst cooler. The changes of heat-transfer coefficient with superficial gas velocity and the ratio of the flow rates from the two gas distributors, that is, u_2/u_1, as well as the increment

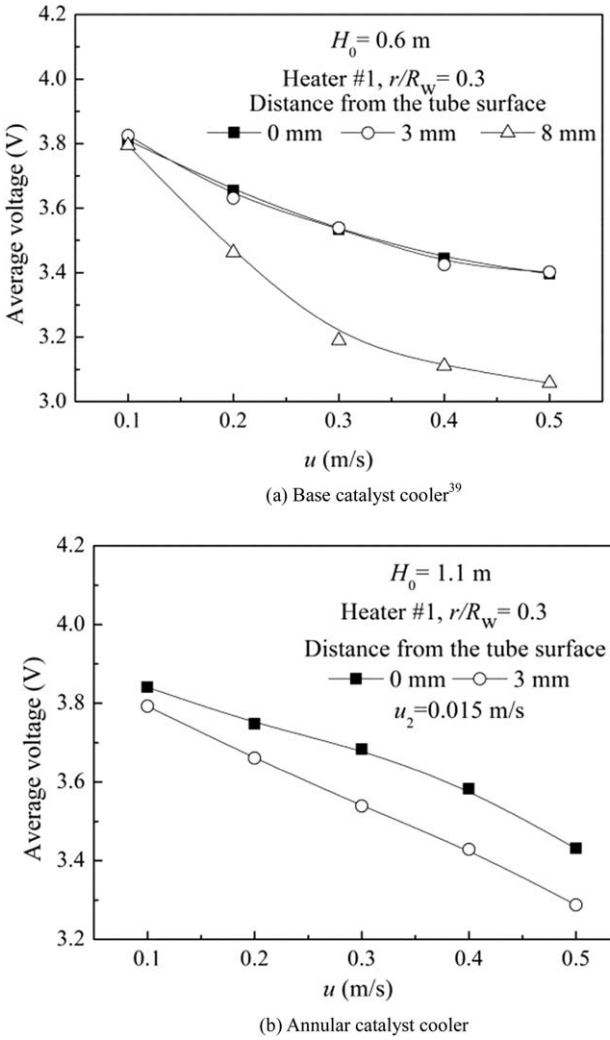

Figure 5. Different thicknesses of static layer on heat tube surface in the two catalyst coolers.

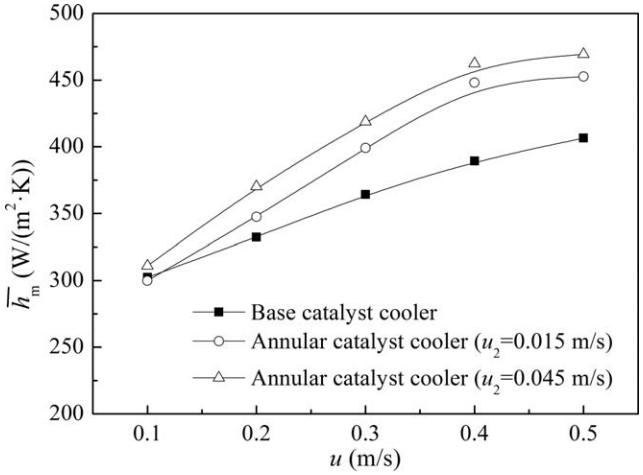

Figure 6. Comparison of total heat-transfer coefficient in the two catalyst coolers.

percentage of heat-transfer coefficient are all agreeable with our previous study.[46] Again, this proved the effectiveness of the new heat transfer intensification method shown in Figure 10. Moreover, despite of the more uniform gas distribution in the base catalyst cooler in this study, the heat transfer intensification effect can still be remarkably seen in the annular catalyst cooler. This further proved that it is the enhanced solids internal circulation, not the improved fluidization quality that plays a dominant role in intensifying the bed-to-wall heat transfer in the annular catalyst cooler.

Effective heat transfer intensification height

Figure 7 compares the axial profiles of heat-transfer coefficient averaged radially by Eq. 6 in the two catalyst coolers at different superficial gas velocities. In the base catalyst cooler, the measured heat-transfer coefficients at different heights are almost same or have only small differences at all superficial gas velocities. That is to say, there are very small axial gradients in its axial profiles of heat-transfer coefficient. In the annular catalyst cooler, there are clear axial gradients of heat-transfer coefficients as shown in Figure 7, especially in the bed bottom. This axial gradient decreases with increasing bed height and increasing superficial gas velocity. Moreover, further increasing u_2/u_1 can also increase its axial gradient of heat-transfer coefficient.

At a low superficial gas velocity, for example, at $u = 0.1$ m/s, the heat-transfer coefficients of the two catalyst coolers show no significant difference at all axial heights. As superficial gas velocity increases, the heat-transfer coefficients of the annular catalyst cooler gradually exceed those of the base catalyst cooler, especially in the bottom bed section. The effects of superficial gas velocity and u_2/u_1 are both agreeable with the results shown in Figure 6. In the bed top, there are no significant increment of heat-transfer coefficient in the annular catalyst cooler even at the highest u and u_2. This demonstrates that the heat transfer intensification effect in the annular catalyst cooler takes effect predominantly in a certain height above the bottom gas distributors. It is believed that the special double-distributor design in the annular catalyst cooler can only affect a certain bed height, above which the enhanced solids circulation shown in Figure 1 and solids renewal on heat tube surfaces will not be remarkable. That is to say, the effect of distributor design weakens with increasing bed height. If the axial height is high enough, there will be no significant difference in the local bed hydrodynamics and heat-transfer properties in both base and annular catalyst cooler as shown in Figure 7.

In a previous study,[46] we found that the tube wall temperature decreased with increasing bed height in the base

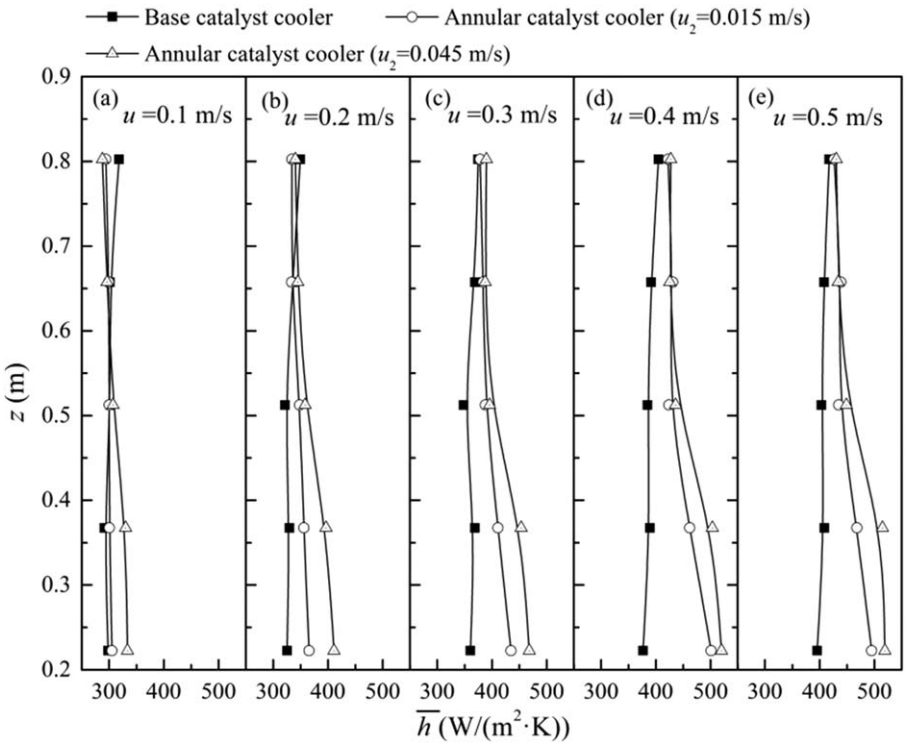

Figure 7. Axial profiles of radial average heat-transfer coefficients.

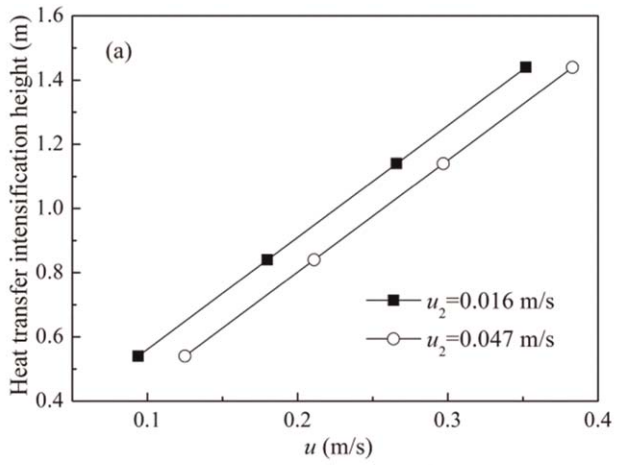

(a) Determined from Yao et al. [46]

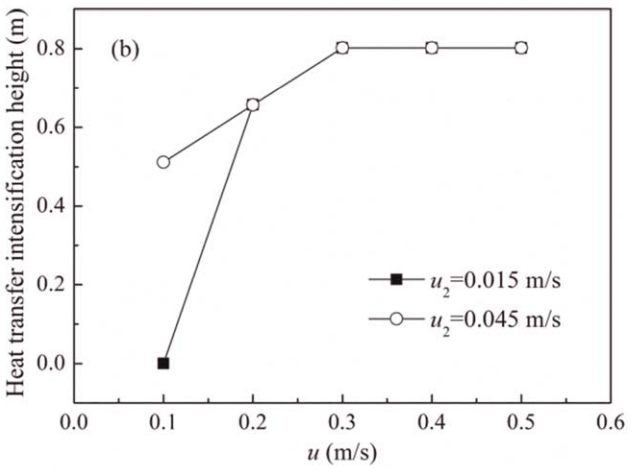

(b) Determined by Figure 7

Figure 8. Comparison of the determined heat transfer intensification heights in Yao et al.[46] and this study.

catalyst cooler as the hot water flowed from the bottom to the top of a heat tube. In the annular catalyst cooler with similar geometrical design to that in this study, different profile of tube wall temperature was found. There existed a minimal value at some operating conditions. A heat transfer intensification height was thus speculated, above which we believe the heat transfer intensification method might be ineffective. Moreover, we also found this heat transfer intensification height increased with increasing superficial gas velocity. The results shown in Figure 7 further prove the existence of the heat transfer intensification height.

Figure 8 compares the heat transfer intensification heights determined based on the results of Yao et al.[46] and this study. Yao et al.[46] defined the heat transfer intensification height as the distance between the bottom plate distributor and the minimal value of heat tube temperature. In this study, the heat transfer intensification height was defined as the distance between the intersection point, which is obtained by the axial curves of heat-transfer coefficient of the two catalyst coolers shown in Figure 7, and the bottom plate distributor. Although the two methods are different physically, the determined heat transfer intensification heights both increase with increasing superficial gas velocity. This further demonstrates that our previous speculation is reasonable.

As seen in Figure 7, the heat transfer intensification is more pronounced in the annular catalyst cooler within a distance of 0.5–0.7 m above the bottom plate distributor. In view of the large dense bed height in industrial FCC external catalyst coolers, a modification is suggested in Figure 9 to further improve the intensification effect of the annular catalyst cooler. It is seen that multiple smaller ring pipe distributors are arranged above the bottom ring pipe distributor. Their functions are to maintain a good fluidization state for the interstitial solids between heat tubes and the cooler wall. These solids are very easy to be defluidized due to stronger wall effect and gas escaping to the bed center. The distances among pairs of the pipe ring distributors should be comparative to the determined heat-transfer coefficient in this study. Ideally, multiple annular catalyst coolers are expected to form in this high industrial FCC catalyst cooler and better heat transfer intensification effect can be obtained.

Comparison of the radial profiles of heat-transfer coefficient and packet parameters

According to the axial profiles of average heat-transfer coefficient shown in Figure 7, the strongest heat transfer intensification effect of the annular catalyst cooler locates in the bed bottom, where Heaters #1 and #2 were positioned. Therefore, the radial profiles of heat-transfer coefficient measured by Heater #1 are selected here to demonstrate the different radial profiles of heat-transfer coefficient in the two catalyst coolers.

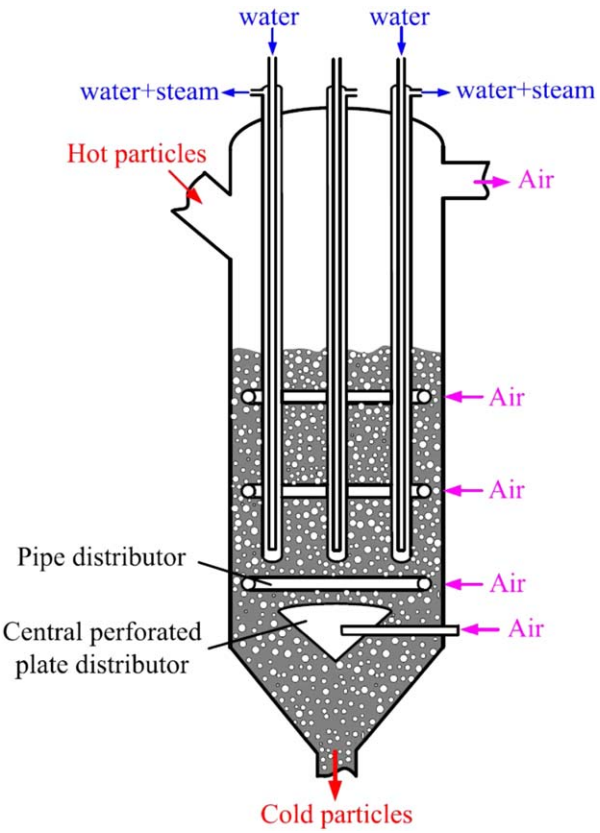

Figure 9. Modified design of the annular catalyst cooler for industrial FCC units.

[Color figure can be viewed in the online issue, which is available at wileyonlinelibrary.com.]

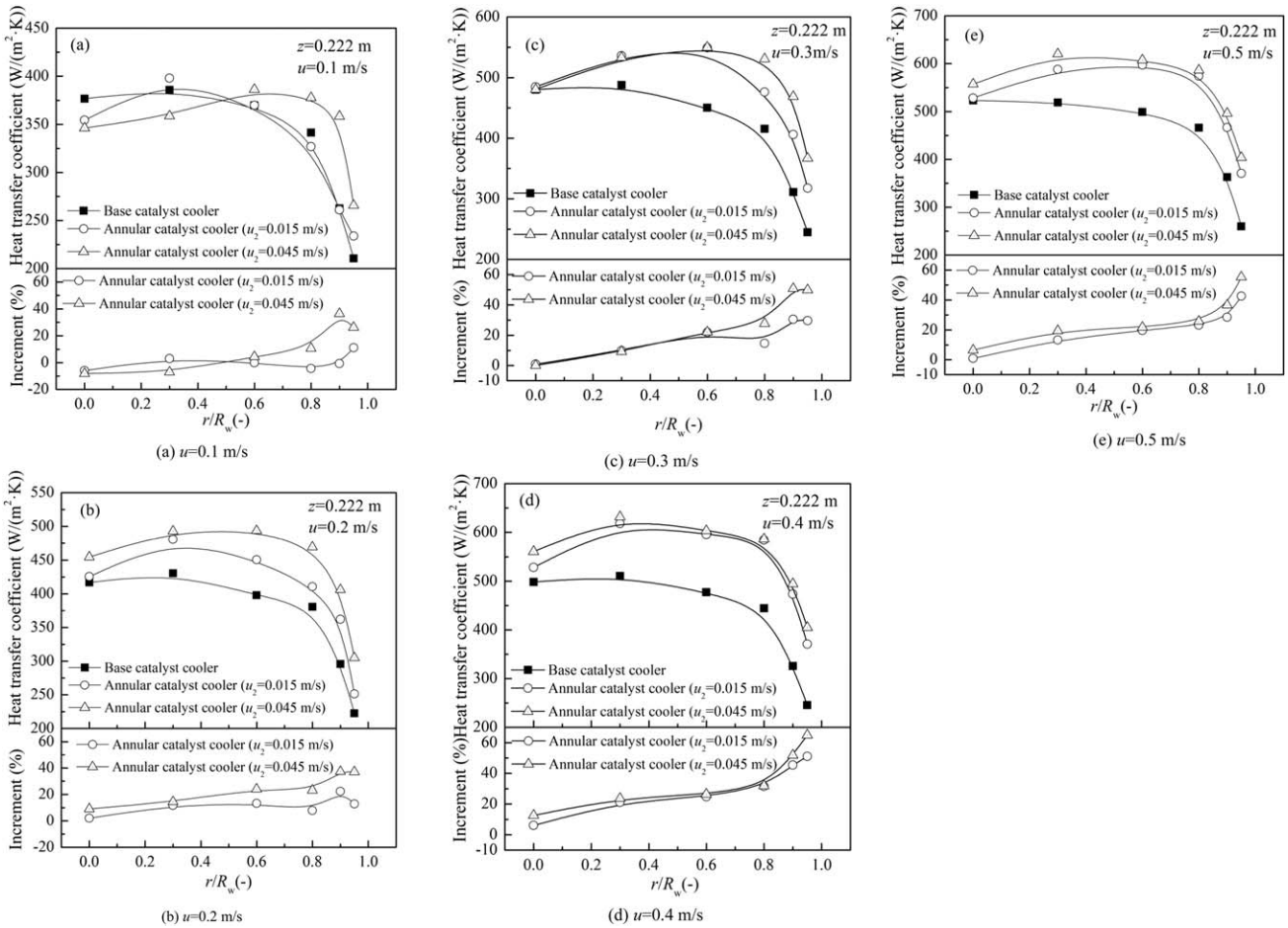

Figure 10. Effect of gas velocity on radial profiles of heat-transfer coefficient.

Figure 10 compares the different radial profiles of heat-transfer coefficient in the two catalyst coolers at different superficial gas velocities. The relative increments of heat-transfer coefficient of the annular catalyst cooler than the base catalyst cooler are drawn in the bottom of each sub figure.

As seen in Figure 10, the profiles of heat-transfer coefficients in the two catalyst coolers are similar in trend, that is, high in the bed center and decreasing sharply as approaching to the column wall. When superficial gas velocity is low, for example, at $u = 0.1$ m/s, there is only small difference between the two catalyst coolers, especially at $u_2 = 0.015$ m/s. At $u_2 = 0.045$ m/s, higher heat-transfer coefficients have already been seen in the annular catalyst cooler as seen in Figure 10a. Considering the measurement errors, the heat intensification effect is in fact not remarkable at $u = 0.1$m/s. This trend can also be observed in the relative increment figure of heat-transfer coefficient in Figure 10a.

At higher superficial gas velocities, for example, at $u \geq 0.2$ m/s, the heat transfer intensification effect of the annular catalyst cooler can already be clearly observed in the radial profiles of heat-transfer coefficients shown in Figures 10b-e. The measured heat-transfer coefficients at all radial positions in the annular catalyst cooler are all higher than in the base catalyst cooler. At $r/R_w > 0.3$, the increments in heat-transfer coefficient in the annular catalyst cooler are more clearly. The relative increment of heat-transfer coefficients increases with increasing r/R_w. When r/R_w is greater than 0.8, all curves of the relative increment of heat-transfer coefficient shown in Figures 10b-e have a steep increase. Moreover, increasing u_2/u_1 will further increase the measured heat-transfer coefficient in the annular catalyst cooler and its effect is also more clearly seen at $r/R_w > 0.8$. This trends described above are all agreeable with Figure 7. The radial profiles of heat-transfer coefficient in the bed center, for example, at $r/R_w < 0.8$, in the two catalyst coolers are also different. The measured h decreases gradually with increasing r/R_w in the base catalyst cooler and increases gradually with increasing r/R_w in the annular catalyst coolers.

The different profiles of heat-transfer coefficient in the annular catalyst cooler are closely related to its different tube surface hydrodynamics. Due to the stronger solids circulation as a result of nonuniform gas distribution, solids renewal on the tube surface is more frequent. This contributes to its higher measured heat-transfer coefficients. Therefore, a precondition of the better heat-transfer performance of the annular catalyst cooler is its special solids circulation pattern and stronger internal solids circulation. Ideally, this requires that all solids in the bed should be well fluidized to guarantee good solids flowability. If defluidization zones or zones with bad fluidization quality exist (e.g., near the wall), the solids circulation will be disrupted and the heat-transfer intensification effect will be impaired. At a low superficial gas velocity, for example, $u = 0.1$ m/s, the nonuniformity of gas distribution and the whole fluidization quality of the bed are not good enough to maintain a stable annular solids

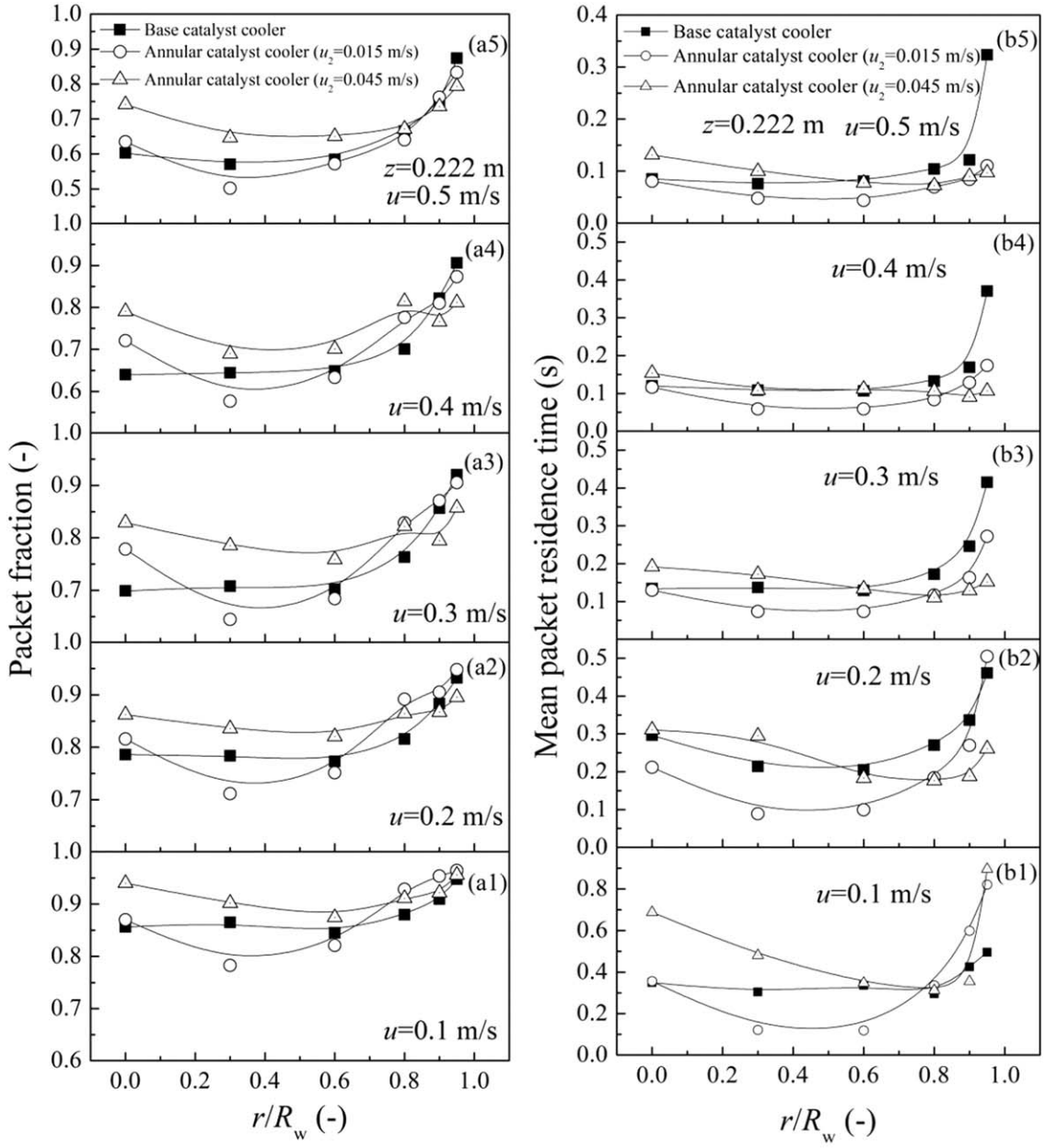

(a) Packet fraction (b) Mean packet residence time

Figure 11. Radial profiles of packet parameters.

circulation and a high circulation rate. That is why the heat-transfer intensification is weak here. Moreover, the increasing of u_2 improved the fluidization quality near the wall, so a higher solids circulation rate can be obtainable. Therefore, the measured heat-transfer coefficient is higher at a higher u_2. The different trend in the radial profiles of heat-transfer coefficient in the annular catalyst cooler at $r/R_w < 0.8$ is also expected to be related to its specified inner hydrodynamics.

Figure 11 presents the radial profiles of packet fraction and mean packet residence time measured at Heater #1 at different superficial gas velocities. Usually, it is believed by most researchers in the fluidization community that the two-phase structure (e.g., bubble and packet in this study) can be successfully detected. However, the measurement errors of particle concentration by fiber optical probes are often believed to be high due to the instability of light source, the nonlinearity between light strength and particle concentration, particle adhesion on the probe tip, and so forth.[49,50] In this study, the measurement error was further enlarged in determining the packet parameters. However, same measurement and data processing methods were adopted in the two catalyst coolers of this study. During discussing the measurement results, the general trends in the experimental data were more emphasized.

As seen in Figure 11a, there is little difference in the radial profiles of packet fraction in the base and annular catalyst coolers at $u_2 = 0.015$ m/s. However, higher packet fractions are seen for the annular catalyst cooler at a higher u_2 of 0.045 m/s. The radial profiles of the measured mean packet residence time are a little messy at $r/R_w \leq 0.8$, but the measured values for the two catalyst coolers in this region, except at $u = 0.1$ m/s, are very adjacent despite of some

fluctuations. However, the profiles of the measured mean packet residence time at $r/R_w > 0.8$ and $u \geq 0.2$ m/s show agreeable trends with the measured radial profiles of heat-transfer coefficient shown in Figures 10b-e. As seen in Figures 11b2–b5, lower mean packet residence times are seen for the annular catalyst cooler. Moreover, the mean packet residence times decrease to lower values when u_2 increases from 0.015 to 0.045 m/s. According to the packet renewal theory,[40] both lower mean packet residence time and higher packet fraction are favorable to higher bed-to-wall heat-transfer coefficient. Moreover, the decreasing of the mean packet residence time, as discussed in our previous study,[46] plays a dominant role in bed-to-wall heat transfer in bubbling fluidized beds as in this study. It further demonstrates the feasibility of the measurement method on heat tube hydrodynamics in this study. For the role in intensifying heat transfer in the annular catalyst cooler, it can thus be concluded from Figure 11 that the reduced mean packet residence time is undoubtedly dominant at $r/R_w \geq 0.8$. At $r/R_w < 0.8$, the intensification effect may be a combined result of the increased packet fraction and reduced mean packet residence time.

Comparison of the axial profiles of heat-transfer coefficient and packet parameters

According to the radial profiles of heat-transfer coefficient, the most pronounced heat transfer intensification effect of the annular catalyst cooler is found at $r/R_w > 0.8$. In the following, we select a radial position and a typical superficial gas velocity as an example to see whether the measured axial profiles of heat-transfer coefficient and packet parameters are agreeable. Figure 12 compares the measured axial profiles of heat-transfer coefficient, packet fraction and mean packet residence time at $r/R_w > 0.8$ and $u = 0.3$ m/s in the two catalyst coolers. The axial profiles of heat-transfer coefficient shown in Figure 12a is similar to Figure 7c, but the increment of heat-transfer coefficient of the annular catalyst cooler is more remarkable. This is easy to understand, as the selected radial position is located in the strongest heat transfer intensification region of the annular catalyst cooler. The bottom region at $z < 0.5$ m has a stronger heat transfer intensification effect. The effect of u_2/u_1 on heat-transfer coefficient is also found to be more pronounced at $z < 0.5$ m.

The axial profiles of packet fraction shown in Figure 12b are a little messy and not agreeable with Figure 12a according to the packet renewal theory.[40] However, the axial profiles of mean packet residence time shown in Figure 12c are agreeable with Figure 12a. Smaller mean packet residence times are measured in the annular catalyst cooler, which corresponds to more frequent packet renewal on the heat tube surface. Moreover, increasing u_2 also leads to decreased mean packet residence time, that is, higher packet renewal frequency. This is also agreeable with Figure 12a. It is a little pity that the agreement between the axial profile of mean packet residence time and that of the heat-transfer coefficient are not so good. The effect of packet fraction on bed-to-wall heat transfer has been proved to be much weaker than packet renewal, as discussed above and in Yao et al.,[39] where we also found that only the trends in the measured mean packet residence times are agreeable with those of heat-transfer coefficient. Therefore, it is not surprising for the disagreements between profiles of packet fraction and heat-transfer coefficient here. Except for the minor role of packet fraction, measurement errors and the inaccurate description of the effect of packet fraction in the packet renewal mechanism,[40] as discussed in Yao et al.,[39] may also contribute to the disagreements. In Yao et al.,[39] we concluded that it was the packet renewal that played a dominant role in bed-to-wall heat transfer in bubbling fluidized beds of fine Geldart A particles. The results presented in Figure 12 can also draw similar conclusions.

Effect of superficial gas velocity on heat-transfer coefficient and packet parameters

In the following, the measured heat-transfer coefficients and packet parameters at different superficial gas velocities

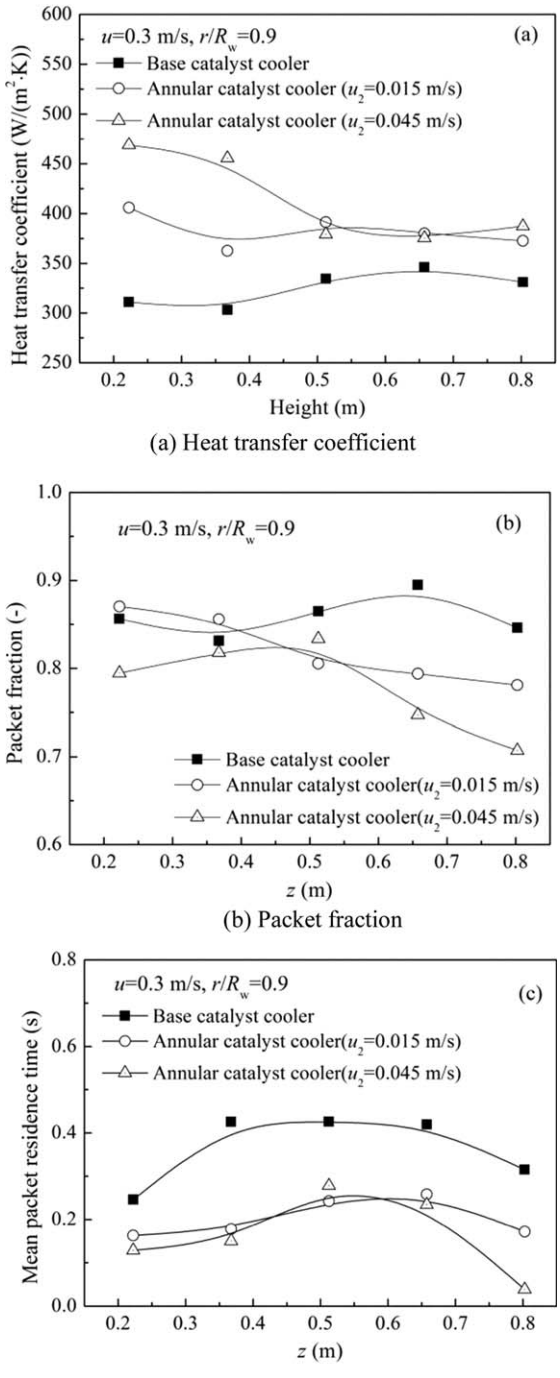

Figure 12. Axial profiles of heat-transfer coefficient and packet parameters.

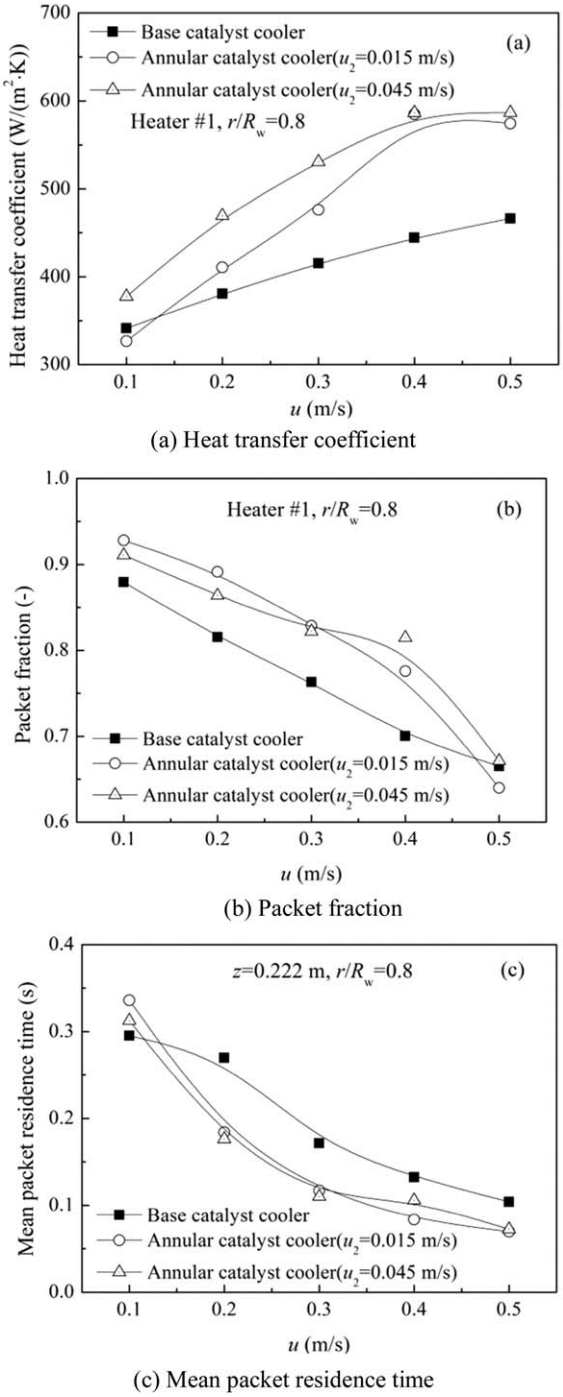

Figure 13. Effect of gas velocity on heat-transfer coefficient and packet parameters.

in a bottom heater (i.e., Heater #1) at $r/R_w = 0.8$ are used as an example to see whether they are agreeable according to the packet renewal theory.[40] Figure 13 compared the three measured parameters at different superficial gas velocities in the two catalyst coolers.

As shown in Figure 13a, heat-transfer coefficients of the two catalyst coolers both increase with increasing superficial gas velocity. Higher measured heat-transfer coefficients are obtained in the annular catalyst cooler. Comparing with the base catalyst cooler, the increment of heat-transfer coefficient of the annular catalyst cooler increases with increasing superficial gas velocity. Higher u_2 also leads to higher heat-transfer coefficient in the annular catalyst cooler. These trends are all agreeable to the total heat-transfer coefficient plotted in Figure 6.

Figure 13b compares the measured packet fraction in the two catalyst coolers. It is found that the packet fraction is higher in the annular catalyst cooler than that in the base catalyst cooler. However, as the effect of packet fraction on bed-to-wall heat transfer is not important, we do not discuss too much here. Figure 13c compares the mean packet residence time in the two catalyst coolers. The mean packet residence times are all found, except at $u = 0.1$ m/s, to be lower in the annular catalyst cooler. This means higher solids renewal frequency on tube surfaces and corresponds to higher heat-transfer coefficient. Increasing u_2 results in lower mean packet residence time in the annular catalyst cooler. These trends are also agreeable with Figure 13a.

Further discussion

The new heat transfer intensification method verified in this study, together with the modified design of an industrial catalyst cooler shown in Figure 9, is expected to be beneficial in three aspects to industrial FCC units. First, for designing a new external catalyst cooler, the annular catalyst cooler is expected to, due to its higher heat-transfer coefficient and smaller required heat-transfer area, be smaller than a traditional cooler as the cooling load is fixed. This means a saving of equipment cost. Second, for an existing catalyst cooler, the upper limit of its cooling capacity is expected to increase by replacing its bottom gas distributor by a double-distributor design guided by the idea of the annular catalyst cooler in this study. This is especially useful when debottlenecking the cooling capacity is necessary in some RFCC units. Due to the bottleneck in the cooling capacity, some RFCC units must reduce throughput or process lighter feedstock. Finally, the usage of high-pressure compressed air, whose pressure is usually higher than the air from the main regenerator blower, is expected to be lower for both cases in the annular catalyst cooler. This also means some energy saving.

Conclusions

In this study, experiment was conducted in a specially designed small cold model to investigate the heat transfer intensification mechanism of a new fluidized catalyst cooler (i.e., the annular catalyst cooler called in this study). Further insights were obtained through the detailed measurements on the axial and radial profiles of heat-transfer coefficient and the tube surface hydrodynamic parameters (i.e., packet fraction and mean packet residence time) by an electrically heated tube and an optical fiber probe in the base and annular catalyst coolers. The following conclusions can be drawn:

1. The measured higher total heat-transfer coefficient further validated the heat transfer intensification method used in the design of the annular catalyst cooler. It was found that the induced higher packet renewal frequency due to the nonuniform gas distribution played the dominant role in its improved heat-transfer performance.

2. Stronger heat transfer intensification effect was found in the bottom of the new fluidized catalyst cooler. The effective heat transfer intensification height speculated previously in our study[46] was confirmed by the measured axial profiles

of heat-transfer coefficient, which was found to increase with increasing gas velocity.

3. In the bed bottom, the annular catalyst cooler showed remarkable heat transfer intensification effect in all radial positions at $u \geq 0.2$ m/s. Compared to the base catalyst cooler, the relative increment of heat-transfer coefficient of the annular catalyst cooler to its base counterpart increased with increasing r/R_w. The strongest intensification effect was seen at an annular near-wall region of $r/R_w > 0.8$.

4. The changes of the measured mean packet residence time in the radial and axial directions and with superficial gas velocity were all found to be agreeable with the measured heat-transfer coefficients according to the packet renewal theory.[40] This further demonstrated the dominant role of packet renewal on bed-to-wall heat transfer and the feasibility of the used experimental method for tube surface hydrodynamics.

5. The new heat transfer intensification method is expected to be beneficial to industrial FCC units in saving equipment cost, increasing throughput, processing heavier feedstock, and decreasing energy consumption.

Acknowledgment

The authors acknowledge the financial supports by the National Natural Science Foundation of China (21276273), the Ministry of Science and Technology of China (2012CB215004), the Ministry of Education of China by the Program for New Century Excellent Talents in University (NCET-11-0733), and the Science Foundation of China University of Petroleum, Beijing (KYJJ2012-03-11).

Notation

A_w = area of heat transfer surface, m^2
h = bed-to-wall heat transfer coefficient, W/(m^2 K)
$\overline{h_{ri}}$ = area-averaged heat transfer coefficient at an axial height, W/(m^2 K)
$\overline{h_m}$ = total average heat transfer coefficient, W/(m^2 K)
H_0 = static bed height, m
n = number of packet identified, -
q = cooling capacity, W
q_{in} = input power by the heating wire, W
r = radial position, m
R_h = resistance of a heating wire, Ω
R_i = radius of fluidized bed, m
R_w = maximum radial position that the heater tube can reach, that is, R_i minus the radius of the heat tube, m
t = total sampling time, s
T_b = bed temperature, °C
T_w = heat tube wall temperature, °C
u = superficial gas velocity, m/s
u_1 = gas flow rate from the central perforated plate distributor divided by the cross-section area of the annular catalyst cooler, m/s
u_2 = gas flow rate from the side ring pipe distributor divided by the cross-section area of the annular catalyst cooler, m/s
U_h = input voltage of a heating wire, V
z = distance from the plate distributor, m

Greek symbols

δ_{pa} = packet fraction, dimensionless
τ_{pa} = mean packet residence time, s
$\tau_{pa,i}$ = residence time of a packet, s

Literature Cited

1. Wilson JW. *Fluid Catalytic Cracking Technology and Operations*. Tulsa, OK: PennWell Publishing Company, 1997.
2. Xu C, Yang Z. *Petroleum Refining Engineering*, 4th ed. Beijing: Petroleum Industry Press, 2009 (in Chinese).
3. Lu C, Wang Z. Fluid Catalytic Cracking Fluidization Technology. Beijing: China Petrochemical Press, 2002 (in Chinese).
4. Lengemann RA. FCC process with dual function catalyst cooling. *US Pat. US5800697*, 1998.
5. Lomas DA, Thompson GJ. *Fluid particle cooling process and apparatus. US Pat. US4434245A*, 1984.
6. Lai Z. Catalyst cooling techniques in heavy oil FCCU. *Pet Ref Eng*. 1995;25(6):44–48 (in Chinese).
7. Chen J. Catalytic Cracking Process and Engineering, 2nd ed. Beijing: China Petrochemical Press, 2005:1338–1343 (in Chinese).
8. Letzsch W. Process and apparatus for controlling catalyst temperature in a catalyst stripper. *US Pat. US7273543B2*, 2007.
9. Lai Z. *Catalyst cooling techniques in heavy oil FCCU. Pet Ref Eng*. 1995;25(6):44–48 (in Chinese).
10. Zhang Y, Qi Y, Li S, Shen J, Yuan X, Wang F. The technology of catalyst cooler in RFCCU and its progress. *J Fushun Pet Inst*. 2002; 22(3):22–26 (in Chinese).
11. Shi B. Classification and heat transfer analysis of external cooler in regenerator of FCCU. *Pet Ref Eng*. 1999;29(11):19–23 (in Chinese).
12. Han J. Discussion of design of catalyst cooler in FCCU. *Catal Crack*. 1998;6:24–30 (in Chinese).
13. Cetinkaya IB, Lomas DA. Heat exchanger with backmix and flow-through particle cooling. *US Pat. US5027893*, 1991.
14. Lomas DA, Thompson GJ. Fluid particle backmixed cooling apparatus. *US Pat. US4483276*, 1984.
15. Anderson LR, Kim HS, Park TG, Ryu HJ, Jung SJ. Operations adjustments can better catalyst-cooler operations. *Oil Gas J*. 1999;97:53–56.
16. Fu S, Zhang J, Geng D. Failure analysis and precaution measures for heat exchange tube bundles in RFCC catalyst cooler. *Chem Eng Equip*. 2011;1:103–107 (in Chinese).
17. Zhou H. Failure analysis and structural improvement of the tube bundle of an FCC external catalyst cooler. *Catal Crack*. 1998;17:28–30 (in Chinese).
18. Gu Y, Li Q, Li L. Analysis of thermal stress of catalyst cooler finned tubes and optimization of construction. *Pet Ref Eng*. 2009;39: 36–41 (in Chinese).
19. Sun F, Zhai X, Yang X, Yang F. Failure analysis to heat removing tube of external heat collector and prevention. *Pressure Vessel Technol*. 2004;21(4):47–49 (in Chinese).
20. Cocco R, Issangya A, Karri SBR, Knowlton T. Understanding streaming flow in deep fluidized beds. *AIChE Annual Meeting: Particle Technology Forum*, San Francisco, USA, 2006.
21. Issangya AS, Knowlton TM, Karri SBR. Detection of gas bypassing due to jet streaming in deep fluidized beds of Group A particles. In: Bi HT, Pugsley T, editors. *Fluidization XII - New Horizons in Fluidization Engineering*. California, USA: Berkeley Electronic Press, 2007:775–782.
22. Karri SBR, Issangya AS, Knowlton TM. Gas bypassing in deep fluidized beds. In: Arena U, Chirone R, Miccio M, Salatino P, editors. *Fluidization XI-Present and Future for Fluidization Engineering*, New York, USA: United Engineering Foundation, 2004:515–521.
23. Wells JW. Streaming flow in large scale fluidization. *AIChE Annual Meeting: Particle Technology Forum*, Reno, Nevada, USA, 2001.
24. Baskakov AP, Berg BV, Vitt OK, Filippovsky NF, Kirakosyan VA, Goldobin JM, Maskaev VK. Heat transfer to objects immersed in fluidized beds. *Powder Technol*. 1973;8(5–6):273–282.
25. Kunii D, Levenspiel O. *Fluidization Engineering*, 2nd ed. New York: Butterworth - Heinemann, 1991.
26. Jin Y, Zhu J, Wang Z, Yu Z. *Fluidization Engineering Principles*. Beijing: Tsinghua University Press, 2001.
27. Wang X. Damage reasons for tube bundle of outside heat remover in heavy oil catalytic cracking unit. *Petrochem Technol Appl*. 2001; 19(3):161–163 (in Chinese).
28. Zhou H. Failure analysis and structural improvement of the tube bundle of an FCC external catalyst cooler. *Catal Crack*. 1998;17(7): 28–30 (in Chinese).
29. Wang H, Chai Z, Zheng T. Analysis of pneumatic controlled external catalyst cooler in FCC unit. *Pet Ref Eng*. 2003;33(11):12–14 (in Chinese).
30. Wang C, Wan D, Wang N, Sun H. Heat transfer analysis of external catalyst cooler in FCC. *Contemp Chem Ind*. 2010;(5):611–613 (in Chinese).
31. Zhang F, Li Z, Pi Y, Shi B. An external catalyst cooler with aeration controlled solids circulation. *Chin Pat. CN 1015901B*, 1990 (in Chinese).
32. Gu Y, Hao X, Li L, Li Q, Tang F. A finned heat tube and an external catalyst cooler with the finned heat tubes. *Chin Pat. CN 201229140Y*, 2008 (in Chinese).

33. Zhang R, Zhang R. Development and application of a dense phase FCC catalyst cooler with enhanced heat-transfer capacity. *Pet Process Petrochem*. 2006;37:50–54 (in Chinese).
34. Jin Y, Wei F, Wang Y. Effect of internal tubes and baffles. In: Yang WC, editor. *Handbook of Fluidization and Fluid-Particle Systems*. New York: Marcel Dekker, Inc., 2003:171–200.
35. Rüdisüli M, Schildhauer TJ, Biollaz S, van Ommen JR. Radial bubble distribution in a fluidized bed with vertical tubes. *Ind Eng Chem Res*. 2012;51(42):13815–13824.
36. Stefanova A, Bi HT, Lim CJ, Grace JR. Heat transfer from immersed vertical tube in a fluidized bed of group A particles near the transition to the turbulent fluidization flow regime. *Int J Heat Mass Transfer*. 2008;51(7–8):2020–2028.
37. Stefanova A, Bi HT, Lim CJ, Grace JR. Local hydrodynamics and heat transfer in fluidized beds of different diameter. *Powder Technol*. 2011;212(1):57–63.
38. Hilal N, Gunn DJ. Heat transfer to immersed boundary surfaces in fluidized beds. *Chem Eng Technol*. 2002;25(10):967–973.
39. Yao X, Han X, Zhang Y, Lu C. Systematic study on heat transfer and surface hydrodynamics of a vertical heat tube in a fluidized bed of FCC particles. *AIChE J*. 2015;61(1):68–83.
40. Mickley HS, Fairbanks DF. Mechanism of heat transfer to fluidized beds. *AIChE J*. 1955;1:374–384.
41. Reddy BV, Basu P. Effect of pressure and temperature on cluster and particle heat transfer in a pressurized circulating fluidized bed. *Int J Energy Res*. 2001;25(14):1263–1274.
42. Yew Looi A, Mao QM, Rhodes M. Experimental study of pressurized gas-fluidized bed heat transfer. *Int J Heat Mass Transfer*. 2002; 45(2):255–265.
43. Grewal NS, Menart J, Hajicek DR, Zobeck BJ. Heat transfer to horizontal tubes immersed in a fluidized-bed combustor. *Powder Technol*. 1987;52(2):149–159.
44. Di Natale F, Lancia A, Roberto N. Surface-to-bed heat transfer in fluidised beds: effect of surface shape. *Powder Technol*. 2007; 174(3):75–81.
45. Abid BA, Ali J M, Alzubaidi AA. Heat transfer in gas-solid fluidized bed with various heater inclinations. *Int J Heat Mass Transfer*. 2011;54(9–10):2228–2233.
46. Yao X, Sun F, Zhang Y, Lu C. Experimental validation of a new heat transfer intensification method for FCC external catalyst coolers. *Chem Eng Process*. 2014;75:19–30.
47. Alappat BJ, Rane VC. Solid circulation rate in recirculating fluidized bed. *J Energy Eng*. 2001;127(2):51–67.
48. Liu M, Xie J, Lu C, Wang Z. Theoretical analysis of hydrodynamics in novel gas-solid annulus-spargered airlift loop reactor. *J Chem Ind Eng (China)*. 2008;59(9):2198–2205 (in Chinese).
49. Li X, Yang C, Yang S, Li G. Fiber-optical sensors: basics and applications in multiphase reactors. *Sensors*. 2012;12:12519–12544.
50. Horio M, Kobylecki RP, Tsukada M. Instrumentation and measurements. In: Yang W-C., editors. *Handbook of Fluidization and Fluid-Particle Systems*. New York: Marcel Dekker, 2003.

Manuscript received Oct. 26, 2014, and revision received Mar. 5, 2015.